Available online at www.sciencedirect.com

ScienceDirect

Physics Procedia 47 (2013) 150 – 155

Physics Procedia

Scientific Workshop on Nuclear Fission Dynamics and the Emission of Prompt Neutrons and Gamma Rays, Biarritz, France, 28-30 November 2012

Measurement of the ^{240,242}Pu neutron-induced fission cross sections

P. Salvador-Castiñeira[a,b,*], R. Bevilacqua[a], T. Bryś[a], F.-J. Hambsch[a], S. Oberstedt[a], C. Pretel[b], M. Vidali[a]

[a]*European Commission - Joint Research Centre - Institute for Reference Materials and Measurements, Retieseweg 111, B-2440 Geel, Belgium*
[b]*Institute of Energy Technologies, Technical University of Catalonia, Avda. Diagonal 647, E-08028 Barcelona, Spain*

Abstract

The neutron-induced fission cross section of ^{240,242}Pu has been measured at the Van de Graaff facility of the Institute for Reference Materials and Measurements (JRC-IRMM). A Twin-Frisch Grid Ionization Chamber (TFGIC) has been used in a back-to-back geometry with the secondary standards ^{237}Np and ^{238}U to normalize the cross section. The energy range measured is from 0.2 keV up to 3 MeV. Preliminary results show some discrepancies around 1 MeV for the ^{242}Pu with the ENDF/B-VII.1 evaluation. The spontaneous fission half-life has been measured for both isotopes, too. Preliminary results show reasonable agreement with the recommended values.

Keywords: neutron-induced fission cross section; ^{240}Pu; ^{242}Pu; spontaneous fission; half-life

1. Introduction

The neutron-induced fission cross section of ^{240,242}Pu was included in a report issued by the Nuclear Energy Agency (Salvatores, 2008) where the nuclear data needs for the innovative GEN-IV nuclear power plants were described. Requested target accuracy are 1-3% for ^{240}Pu and 3-5% for ^{242}Pu in the energy region from 500 keV to 2.5 MeV compared to presently 6% and 20%, respectively.

The ANDES collaboration (Accurate Nuclear Data for nuclear Energy Sustainability) has developed a program of specifically targeted actions to address the critical points - such as the improvement of basic measurements of the cross sections of critical reactions of selected isotopes ... - of the knowledge of nuclear data for its application to the development of the nuclear systems and their fuel cycles required to enhance the nuclear energy sustainability. In relation with the neutron-induced fission cross section of ^{240,242}Pu, the present work aims of providing new data taken relative to other standards than ^{235}U, as nearly all other experimental data are relative to the latter one.

* Corresponding author. Tel.: +32-(0)14-573-014; fax: +32-(0)14-571-376.
E-mail address: paula.salvador-castineira@ec.europa.eu

doi:10.1016/j.phpro.2013.06.022

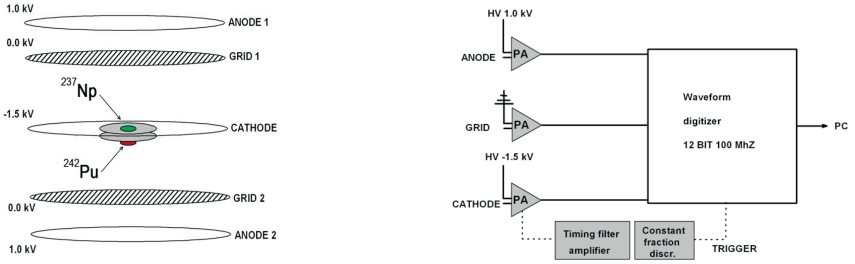

Fig. 1. Schematic drawing of TFGIC with samples placed in a back-to-back geometry for cross section measurements (left) and the corresponding electronic scheme (right).

2. Experimental setup

A Twin-Frisch Grid Ionization Chamber (TFGIC) has been used as fission fragment detector. The advantage of using this detector in a back-to-back geometry is that there is no need of determining the neutron flux impinging the sample under study since it can be assumed to be the same for both samples. The TFGIC was filled with P10 gas (90% Ar + 10% CH_4) at a constant flow rate of ca. 50 ml/min. The pressure was controlled at 1053 mbar. Figure 1 shows a schematic drawing of the TFGIC and its electronic scheme. The anodes and the grids were connected to charge sensitive preamplifiers, while the cathode was connected to a current sensitive one. The cathode was triggering all the system, therefore this signal was processed with a time filter amplifier and a constant fraction discriminator, where an electronic threshold was set for rejecting as many α particles as possible. This trigger was connected to the three boards of the 12 BIT 100 MHz Wave-Form Digitizer (WFD), together with the 5 raw signals from the preamplifiers.

All the samples used in this experiment have been produced by the sample preparation group of JRC-IRMM. Therefore, the precision of the mass and the isotopic content of the samples will help on reaching the target accuracy requested by OECD. Table 1 provides an extended description of the samples used.

Table 1. Description of the samples under study (^{240}Pu and ^{242}Pu) and the secondary standards used (^{237}Np and ^{238}U) (Sibbens et al., 2011; Pommé , 2012).

	^{240}Pu	^{242}Pu	^{237}Np	^{238}U
Method	electrodeposition	electrodeposition		vacuum deposition
Mass (μg)	92.9 (0.4%)	671 (1.2%)	391.3 (0.3%)	614 (0.5%)
Diameter (mm)	29.95 (0.01%)	29.95 (0.01%)	12.7	30
Areal density (μg/cm^2)	13.19 (0.4%)	95.3 (1.2%)	308.9	86.9
Backing	aluminium	aluminium	stainless steel	aluminium
α-activity (MBq)	0.780 (0.4%)	0.0984 (0.8%)	10193×10^{-6} (0.1%)	7.64×10^{-6} (0.5%)
Purity	99.8915*18%*	99.9651*845%*		

3. Cross section measurement

The measurements have been performed at the Van de Graaff facility of the JRC-IRMM. Several campaings have been done for the two plutonium isotopes using the two different standards. The neutron producing reactions used were ^{7}LiF(p,n)^{7}Be for neutron energies between 0.2 keV and 1.8 MeV and using ^{237}Np(n,f) as a reference cross section; and T(p,n)^{3}He for neutron energies between 1.8 and 3 MeV and using ^{238}U(n,f) as a reference. The neutron-induced fission cross section is described as

$$\sigma_{\mathrm{Pu}}(E_n) = \left[\frac{N_{\mathrm{ref}}}{N_{\mathrm{Pu}}}\cdot\frac{(C_{\mathrm{Pu}}-C_{\mathrm{SF}})}{C_{\mathrm{ref}}}\cdot\frac{\epsilon_{\mathrm{ref}}}{\epsilon_{\mathrm{Pu}}}-\sum_i P_i\cdot\frac{\sigma_i(E_n)}{\sigma_{\mathrm{ref}}(E_n)}\right]\cdot\sigma_{\mathrm{ref}}(E_n) \quad (1)$$

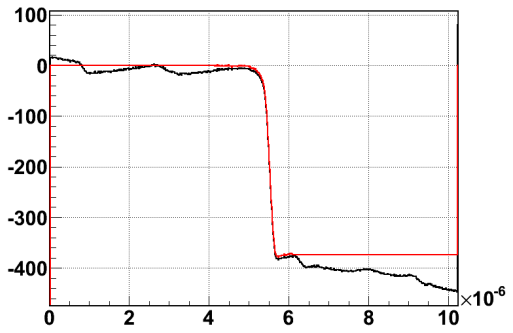

(a) Anode signal after the preamplifier of a FF detected in coincidence with α particles (black) and the same signal after the α pile-up correction (red). Y-axis in mV and X-axis in s.

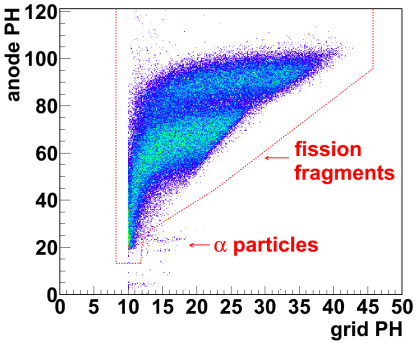

(b) Anode PH vs grid PH. A good discrimination between α particles and FF is observed.

Fig. 2. Difference between the α pile-up correction during the DSP analysis and the α discrimination during the PH analysis.

where N_i are the number of atoms in the sample i, C_i are the number of counts detected from the sample i, C_{SF} are the number of spontaneous fission counts from the plutonium sample, ϵ_i is the transmission probability of a fission fragment (FF) to leave the sample and enter into the counting gas, $\sum_i P_i \cdot \frac{\sigma_i(E_n)}{\sigma_{\mathrm{ref}}(E_n)}$ is the contribution on the plutonium fission counts from the impurities of the sample and $\sigma_{\mathrm{ref}}(E_n)$ is the cross section from the reference isotope. The uncertainty calculation includes the contribution of the sample mass, the uncertainties on the half-life and isotope content, and statistics.

3.1. Digital-Signal Processing (DSP)

As explained above, the preamplifiers were fed into a WFD, where all the traces were recorded for an offline analysis. This analysis was performed by using the novel DSP. The advantages of using this method instead of analogue electronics with high α activated samples is that it is possible to treat traces where α particles were detected in the same time window than a fission fragment (FF). The traces were treated within the scheme: baseline correction, ballistic deficit correction, α pile-up correction and CR-RC^4 filtering. After that, the pulse height (PH) distribution for each electrode is obtained. Figure 2a shows an example of several α particles piled up with a FF.

3.2. Pulse Height Analysis

After having obtained the PH distributions, additional corrections need to be applied, namely: grid inefficiency, α discrimination, sample loss and detector threshold. A detailed exaplanation of each of them follows.

3.2.1. Grid inefficiency correction

The grid inefficiency was explained in detail in Ref. (Al-Adili et al. , 2012).

3.2.2. α discrimination

Previously we have explained how α particles were rejected when they were detected together with a FF. Nevertheless, one needs to consider that several α particles can be detected when the cathode triggers due to a FF in the opposite side of the TFGIC. Those particles can be well recognized if one represents the anode PH against the grid PH (see figure 2b).

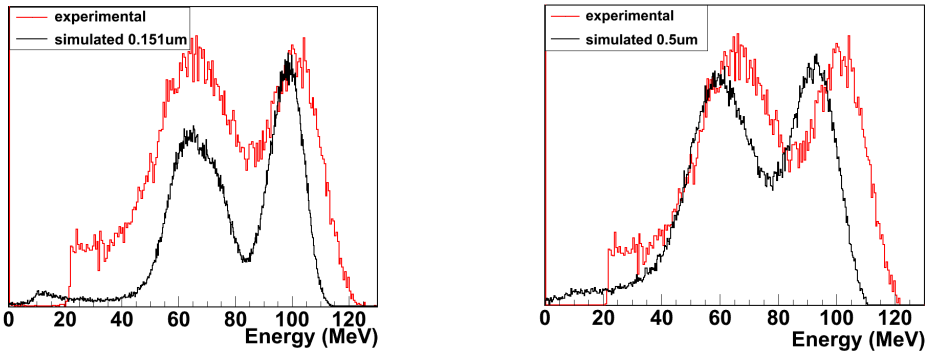

Fig. 3. Comparison between the simulations and the experimental data considering two different thickness of the sample.

3.2.3. Sample loss correction

It is known that due to the finite thickness of the sample some FFs, mostly the ones emitted at large angles, will be stopped within the sample, before entering into the counting gas. Those FFs will not be detected but they need to be considered for the cross section calculation. A first approximation would be to consider a sample of a infinite radius and a finite width. This assumption is possible thanks to the fact that the sample's thickness is several orders of magnitude lower than the sample radius. If one assumes that a FF can be generated at any place of the sample, it is possible to calculate the maximum angle of emission for this FF by knowing the stopping power of the medium where the FF is travelling. The typical FF ranges inside uranium were obtained using the SRIM code (Ziegler et al. , 2008). The transmission probability (ϵ) calculated for each sample is: 98.3% for ^{237}Np, 99.9% for ^{240}Pu and ^{238}U and 99.5% for ^{242}Pu.

Those results are preliminary and need to be improved by means of Monte Carlo simulations.

3.2.4. Detector threshold

To be able to discard as many α particles as possible not to have them triggering the system, the electronic threshold needs to be set to a high level. This means that the low energy FFs will not trigger, as they will be below the threshold. Therefore, several approaches are being under study to account for these FFs: an exponential fit and a three gaussian fit. By considering one or the other, differences around 6% in the final cross section values would be obtained.

To have a better understanding of which is the behaviour of the PH at low energies, we have built a C++ code to simulate the sample and the mounting plate where it is placed. This code uses an input distribution of post-neutron emission FF kinetic energy (KE) and mass number from GEF (Schmidt and Jurado , 2012). Once this information is read by the code, it calculates the ranges using SRIM and finally, calculates the energy deposited of the FF in the gas.

If we plot our results with the experimental data (figure 3), we obtain that the sample should be 4 times thicker. For calculating the neutron-induced fission cross section the exponential fit described previously will be applied to the data.

4. Spontaneous fission measurement

In addition, the spontaneous fission half-life is being under study. The calculation is done by

$$T_{1/2,SF} = \frac{\%^{j}\mathrm{Pu}}{\mathrm{A}_j} \frac{1}{\left(\frac{C_{SF}}{t \cdot \epsilon_j \cdot \ln 2 \cdot m_{\mathrm{Pu}} \cdot N_A} - \sum_{i}^{n} \frac{\%^{i}\mathrm{Pu}}{\mathrm{A}_i \cdot T_{1/2,SF}(i)} \right)} \tag{2}$$

where $\%^{j}$Pu is the purity of the sample, A_j its atomic mass, C_{SF} are the counts detected, ϵ_j is the transmission probability from the sample to the counting gas, m_{Pu} is the sample mass, N_A the Avogadro's number and $\sum_{i}^{n} \frac{\%^{i}\mathrm{Pu}}{\mathrm{A}_i \cdot T_{1/2,SF}(i)}$ the contribution from the other isotopes contained in the sample.

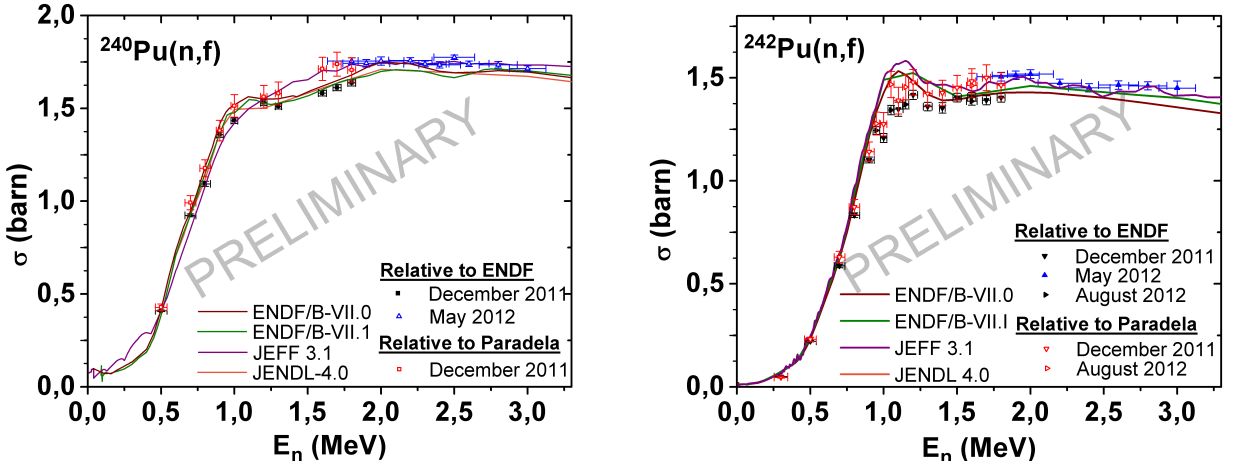

Fig. 4. Preliminary results on the neutron-induced fission cross section for ^{240,242}Pu (see text for further explanation).

5. Results and discussions

The results presented in this section are preliminary.

5.1. Neutron-induced fission cross section

The measurements have been done over several campaings. All the data are being presented. Figure 4 presents the preliminary results on neutron-induced fission cross section for ^{240,242}Pu. Two different normalizations have been performed. At first, the data were normalized to the ENDF/B.VII.1 evaluation (ENDF , 2012) for the two reference isotopes (^{237}Np - black symbols- and ^{238}U - blue symbols-). As it is observed, the main discrepancies are seen at around 1 MeV neutron incoming energy for ^{242}Pu were our data cannot reproduce the resonance-like structure seen in the evaluations. In addition, there is a discrepancy in both isotopes at 1.8 MeV between the data taken relative to ^{237}Np and the one relative to ^{238}U. Recently, new values for the neutron-induced fission cross section for ^{237}Np were published by (Paradela et al., 2010), these data were around 5% higher in value than the current evaluations. By normalizing our ^{237}Np data to (Paradela et al., 2010), the red symbols would be obtained. Then, the resonance-like structure is followed closer for the ^{242}Pu and the values at 1.8 MeV for the two different standards are within uncertainties. Nevertheless, by using (Paradela et al., 2010) our uncertainties would be much larger and will not fulfill the requirements of the project.

5.2. Spontaneous fission half-life

The spontanoeus fission half-life ($T_{1/2,SF}$) is being determined for ^{240,242}Pu. Tables 2 and 3 present the preliminary results obtained by calculating the non-weighted average over some runs. As we can see, the results presented for both isotopes are slightly higher than the reference value given by (Holden and Hoffman , 2000). Those results are strongly dependent on the transmission probability of a FF to leave the sample and enter into the gas and, as well, on the fit done at low KE. Therefore, those values might change once these parameters are better understood.

6. Conclusions

The neutron-induced fission cross section has been measured for ^{240,242}Pu at the Van de Graaff facility of the JRC-IRMM. The energy range studied has been between 0.2 MeV and 3 MeV neutron incoming energy. The preliminary results presented are in agreement with evaluations, but for ^{242}Pu at around 1 MeV where our data cannot reproduce

Table 2. Preliminary results on the SF half-life ($T_{1/2,SF}$) for ^{240}Pu compared with previous experimental values.

	$T_{1/2,SF}$ (y)	Comments
(Budtz-Jorgensen et al. , 1980)	$(1.15 \pm 0.03) \times 10^{11}$	Fragment spectra; ionization chamber. ≈1000 fiss.
(Androsenko et al. , 1984)	$(1.15 \pm 0.03) \times 10^{11}$	Spontaneous fission neutron emission rates
(Selickij et al. , 1988)	$(1.17 \pm 0.03) \times 10^{11}$	Fission fragment detection in 2π geometry
(Ivanov et al. , 1991)	$(1.15 \pm 0.02) \times 10^{11}$	λ_f/λ_α in two ^{240}Pu standards
(Holden and Hoffman , 2000)	$(1.14 \pm 0.01) \times 10^{11}$	Recommended value
This measurement (April '12)	$(1.184 \pm 0.007) \times 10^{11}$	≈50000 fissions · 2 measurements
This measurement (Oct '12)	$(1.207 \pm 0.006) \times 10^{11}$	>110000 fissions · 1 measurement

Table 3. Preliminary results on the SF half-life ($T_{1/2,SF}$) for ^{242}Pu compared with previous experimental values.

	$T_{1/2,SF}$ (y)	Comments
(Meadows , 1977)	$(6.74 \pm 0.05) \times 10^{10}$	λ_α/λ_f rel. total $t_{1/2}(^{239}\text{Pu})$ = 24290 y
(Selickij et al. , 1988)	$(6.86 \pm 0.26) \times 10^{10}$	Fission fragment detection in 2π geometry
(Holden and Hoffman , 2000)	$(6.77 \pm 0.07) \times 10^{10}$	Recommended value
This measurement (November '11)	$(6.97 \pm 0.09) \times 10^{10}$	≈50000 fiss each measurement
This measurement (August '12)	$(6.99 \pm 0.09) \times 10^{10}$	>100000 fiss each measurement

the resonance-like structure seen in the present evaluations. Two different secondary standards have been used: ^{237}Np and ^{238}U. The results obtained at the common neutron energy of 1.8 MeV do not agree within uncertainties. By normalizing the data to the new values of the neutron-induced fission cross section of ^{237}Np (Paradela et al. , 2010) instead of the ENDF/B.VII-1 evaluation, those discrepancies seem to be solved. The SF half-life is being under study, too, and preliminary data show slightly higher values.

Acknowledgements

The authors would like to acknowledge the technicians of the Van de Graaff accelerator at the JRC-IRMM for providing a very good beam and to the sample preparation group for preparing the high quality samples.

References

Al-Adili, A., Hambsch, F.-J., Bencardino, R., Oberstedt, S., Pomp, S., 2012. Ambiguities in the grid inefficiency correction for Frisch-Grid Ionization Chambers. Nuclear Instruments and Methods in Physics Research A 673, 111-121.

Androsenko, A.A., *et al.*, 1984. Sov.J.At.Energy 57, 788.

Budtz-Jorgensen, C., *et al.*, 1980. Euratom Pogr. Rep. NEANDC(E)-212-3,5.

Evaluated Nuclear Data File, 2012. www.nndc.bnl.gov.

Holden, N.E., Hoffman, D.C., 2000. Spontaneous fission half-lives for ground-state nuclides. Pure Appl. Chem., Vol.72, No. 8, pp.1525-1562.

Ivanov, Yu.V., *et al.*, 1991. Sov.J.At.Energy 70, 491.

Meadows, J.W., 1977. Argonne Nat. Lab. Report ANL/NDM-38.

Paradela, C., *et al.*, 2010. Neutron-induced fission cross section of ^{234}U and ^{237}Np measured at the CERN Neutron Time-of-Flight (n_TOF) facility. Phys. Rev. C 82, 034601.

Pommé, S., 2012, private communication.

Salvatores, M., 2008. NEA/WPEC-26, OECD.

Schmidt, K.H. , Jurado, B., 2012, GEF-code version 2.7.

Selickij, Ju.A., Funstein, V.B., Jakovlev, V.A., 1988. Proc. 38th Annual Conf. Nuclear Spectros. and Structure in Atomic Nuclei, Baku, 12-14 Apr., p.131, Acad. Sci. USSR.

Sibbens, G., *et al*, 2011. Preparation of thin layer ^{240}Pu and ^{242}Pu targets at IRMM. WP1 ANDES meeting.

Ziegler, J. F. et al. www.srim.org (v-2008.03)